Int. J. Solids Structures, 1975, Vol. 11, pp. 827–840. Pergamon Press. Printed in Great Britain.

DYNAMICS OF CURVED BEAMS INVOLVING SHEAR DEFORMATION

YAIR TENE,† MARCELO EPSTEIN‡ and IZHAK SHEINMAN§
Faculty of Civil Engineering, Technion-Israel Institute of Technology, Haifa, Israel

(*Received* 25 *April* 1974; *revised* 2 *December* 1974)

Abstract—A general analytical and numerical procedure, based on the linear theory, is outlined for the elastic stress and deflection analysis of an arbitrary plane curved beam subjected to arbitrary static and dynamic loads. The equations of motion admit shear deformation and rotary inertia. The numerical solution is obtained by Houbolt's method and by finite differences. The paper also presents two numerical examples.

NOTATATION

A area
$\mathbf{e}_i$ base vector
E_{ij} strain tensor
E modulus of elasticity
EVW external virtual work
G_{ij} metric tensor
IVW internal virtual work
M bending moment
$\mathbf{N}$ unit normal vector
N axial force
p external load
Q shear force
$\mathbf{r}$ position vector to the axis
$\mathbf{R}$ position vector of any point in the plane
s coordinate along axis
$\mathbf{T}$ unit tangent vector
t time
u tangent displacement
$\mathbf{v}$ displacement vector
w normal displacement
$\mathbf{y}$ displacement vector
z coordinate along normal
κ curvature
$\boldsymbol{\eta}$ vector defined in equation (10)
Φ rotation
σ^{ij} stress tensor
ρ density
$()'$ $d/ds\,()$
$\dot{()}$ $d/ds\,()$

1. INTRODUCTION

The effects of transverse shear deformation and rotary inertia were first introduced in the theory of straight beams by Timoshenko[1]. Using Timoshenko's theory numerical results have been obtained[2] by integration along the characteristics and compared[3] with solutions obtained by two other procedures: normal mode superposition and Houbolt's method[4].

The results of [3] indicate that Houbolt's method can be used with advantage regardless of the history and distribution of the loads, making it suitable for cases of rapidly varying and discontinuous loads which occur often in practice. Houbolt's method has, furthermore, the feature of being stable for any given time differential[5], accuracy being therefore the only consideration involved in the choice of the latter.

Timoshenko's theory has been generalized for the case of thin shells of arbitrary shape[6] and applied for the static analysis of skew plates[7].

In the present work a Timoshenko-type theory is derived for plane curved beams of arbitrary shape. The kinematical unknowns are chosen so as to yield second order differential equations,

†Associate Professor.
‡Lecturer.
§Lecturer.

an advantage from the numerical viewpoint over equations of higher order. A numerical solution procedure is presented based on the application of Houbolt's method and the use of finite differences with interlaced nets for the resulting pseudo-static equations. Two numerical examples are included.

2. ANALYTICAL FORMULATION

Geometry

In a plane beam all material properties, as well as the external loading, are symmetric with respect to a plane containing the axis of the beam. This axis can be chosen arbitrarily, the only limitations being that it must lie in the plane of symmetry and be compatible with the basic kinematic assumption of the theory (see next section).

Let x,y (Fig. 1) be the plane of symmetry and let the axis before deformation be described by the following equation:

$$\mathbf{r} = \mathbf{r}(s) \tag{1}$$

where s denotes axial length.

The following geometrical relations hold at every point of the axis:

$$\mathbf{T} = \frac{d\mathbf{r}}{ds} \tag{2}$$

$$\frac{d\mathbf{T}}{ds} = -\kappa \mathbf{N} \tag{3}$$

$$\frac{d\mathbf{N}}{ds} = \kappa \mathbf{T} \tag{4}$$

where

- $\mathbf{T}$ unit tangent vector co-directional with increasing s,
- $\mathbf{N}$ unit normal vector such that $\mathbf{T}$, $\mathbf{N}$ is counterclockwise,
- κ curvature, $\kappa > 0$ with $-\mathbf{N}$ directed towards the center of curvature.

The position vector of any point in the plane can be given by:

$$\mathbf{R}(s, z) = \mathbf{r}(s) + z\mathbf{N}(s) \tag{5}$$

where z denotes length along the normal.

Equation (5) is in fact a coordinate transformation in the plane. The s, z system of coordinates can be regarded as "natural" for analysis of the curved beam. The base vectors of the system are:

$$\mathbf{e}_1 = \frac{\partial \mathbf{R}}{\partial s} = (1 + \kappa z)\mathbf{T} \tag{6}$$

$$\mathbf{e}_2 = \frac{\partial \mathbf{R}}{\partial z} = \mathbf{N} \tag{7}$$

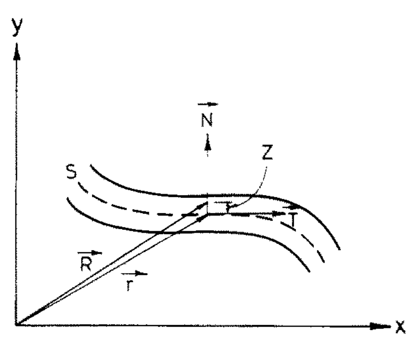

Fig. 1. Plane of symmetry of the beam.

The metric tensor is defined by:

$$G_{ij} = \mathbf{e}_i \cdot \mathbf{e}_j \tag{8}$$

and equation (6) and (7) yield the following equalities for its components:

$$\begin{aligned} G_{11} &= (1 + \kappa z)^2 \\ G_{12} &= G_{21} = 0 \\ G_{22} &= 1 \end{aligned} \tag{9}$$

Kinematics

The basic assumption of the first-order beam theory used here is that plane sections normal to the axis of the beam before deformation remain plane, but not necessarily normal to the axis, after deformation.

For simple mathematical formulation of this hypothesis, s, z are conveniently regarded as convected coordinates, i.e. coordinates attached to the material points of the beam. In other words, each particle lying in the plane of symmetry is identified by a fixed pair of numbers s,z for all values of the time parameter t.

In these circumstances, the position vector $\mathbf{R}(s, z, t)$ of particle s, z at time t is:

$$\mathbf{R}(s, z, t) = \mathbf{r}(s) + \mathbf{v}(s, t) + z\boldsymbol{\eta}(s, t) \tag{10}$$

where

- $\mathbf{v}$ displacement vector of points on the axis,
- $\boldsymbol{\eta}$ vector through the material points that were on $\mathbf{N}$ before deformation (see [6, 7]).

For the initial time t_0, the following equalities hold:

$$\mathbf{R}(s, z, t_0) = \mathbf{R}(s, z) \tag{11}$$

and

$$\boldsymbol{\eta}(s, t_0) = \mathbf{N}(s) \tag{12}$$

In what follows, $\boldsymbol{\eta}$ is assumed a unit vector implying that transverse normal strains are neglected.

According to equation (10), the deformation of the beam is described by the two vector functions $\mathbf{v}$, $\boldsymbol{\eta}$. These functions can be expressed in terms of their components in the initial configuration as follows:

$$\mathbf{v} = u\mathbf{T} + w\mathbf{N} \tag{13}$$

$$\boldsymbol{\eta} = \Phi\mathbf{T} + \alpha\mathbf{N} \tag{14}$$

where u, w, ϕ, α are scalar functions of s and t.

In a linear theory displacements and rotations are considered "small", hence, the projection of $\boldsymbol{\eta}$ on $\mathbf{N}$ is given by the cosine of a "small" angle, namely $\alpha = 1$ and

$$\boldsymbol{\eta} = \Phi\mathbf{T} + \mathbf{N} \tag{15}$$

Substituting equations (13) and (15) into equation (10) and referring to equation (5), we have:

$$\mathbf{R}(s, z, t) = \mathbf{R}(s, z) + (u + z\Phi)\mathbf{T} + w\mathbf{N} \tag{16}$$

The deformation of the beam is thus completely defined by the three scalar functions u, w and ϕ (Fig. 2). Note that in a theory which disregards shear deformations, the vector $\boldsymbol{\eta}$ coincides at every instant with the normal to the axis and ϕ is no longer independent of u and w.

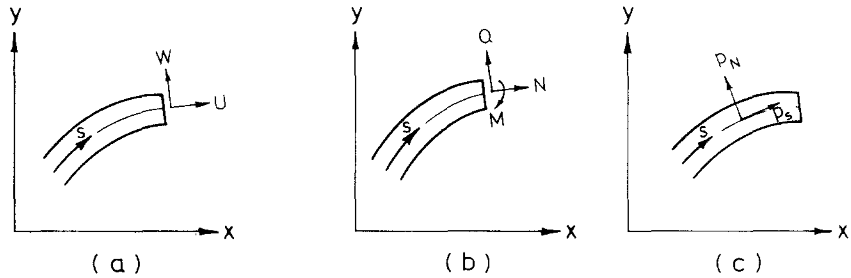

Fig. 2. (a) Displacements; (b) Internal forces; (c) External forces.

The strain tensor is defined as:

$$E_{ij}(s, z, t) = \frac{1}{2}[G_{ij}(s, z, t) - G_{ij}(s, z, 0)] \tag{17}$$

where $G_{ij}(s, z, t)$ is the metric tensor at time t, and $G_{ij}(s, z, 0) = G_{ij}(s, z)$ is given in equations (9).

The base vectors of the system s, z at time t are given by:

$$\mathbf{e}_1(s, z, t) = \frac{\partial \mathbf{R}(s, z, t)}{\partial s} = \mathbf{e}_1 + (u' + z\Phi' + \kappa s)\mathbf{T} + (w' - \kappa u - kz\Phi)\mathbf{N}$$

$$\mathbf{e}_2(s, z, t) = \frac{\partial \mathbf{R}(s, z, t)}{\partial z} = \mathbf{e}_2 + \Phi\mathbf{T} \tag{18}$$

where $()' = \mathrm{d}/\mathrm{d}s\,()$.

Using equations (8), (9) and (18), and neglecting second-order terms in the displacements, the following expressions are obtained for the components of the strain tensor:

$$E_{11}(s, z, t) = u' + \kappa w + z(\Phi' + \kappa u' + \kappa^2 w) + z^2 \kappa \Phi'$$

$$E_{12}(s, z, t) = \frac{1}{2}(\Phi + w' - \kappa u) \tag{19}$$

$$E_{22}(s, z, t) = 0$$

Equations (19) relate the strain tensor with the kinematic unknowns u, w and Φ. E_{12} may be chosen directly as an unknown instead of Φ, but this leads to third-order equations instead of the more convenient second-order equations obtained with the present choice.

Equations of motion

The equations of motion are derived by the principle of virtual displacements which postulates equality of the internal and external virtual work

$$IVW = EVW \tag{20}$$

The internal virtual work is given by:

$$IVW = \int_s \left[\iint_{A(s)} (\sigma^{11}\delta E_{11} + 2\sigma^{12}\delta E_{12})\,\mathrm{d}A\right]\mathrm{d}s \tag{21}$$

where

σ^{ij} stress tensor

$A(s)$ area of section at s.

The external virtual work, incorporating the influence of the inertial forces, is:

$$EVW = \int_s \mathbf{P}(s, t)\delta\mathbf{v}(s, t)\mathrm{d}s - \int_s \left[\iint_{A(s)} \rho\ddot{\mathbf{y}}(s, z, t)\delta\mathbf{y}(s, z, t)\mathrm{d}A\right]\mathrm{d}s \tag{22}$$

where

$\mathbf{p}(s, t)$ external load vector per unit length of axis,
$\mathbf{y}(s, z, t)$ displacement vector of a point in the plane of symmetry of the beam,
ρ density.
$\dot{(\ )}$ $\mathrm{d}/\mathrm{d}t$ ( ).

In terms of their components, $\mathbf{p}$ and $\mathbf{y}$ become:

$$\mathbf{p} = p_s\mathbf{T} + p_N\mathbf{N} \tag{23}$$

$$\mathbf{y} = \mathbf{R}(s, z, t) - \mathbf{R}(s, z) = (u + \Phi z)\mathbf{T} + w\mathbf{N} \tag{24}$$

Substituting equations (24) and (19) into (21) and (22) we obtain:

$$IVW = \int_s \{N\delta u' - \kappa Q\delta u + \kappa N\delta w + Q\delta w' + Q\delta\Phi + M\delta\Phi'\}\,\mathrm{d}s \tag{25}$$

$$EVW = \int_s \{p_s\delta u + p_N\delta w - [I_0\ddot{u} + I_1\ddot{\Phi}]\delta u + [I_1\ddot{u} + I_2\ddot{\Phi}]\delta\Phi + I_0\ddot{w}\delta w\}\,\mathrm{d}s \tag{26}$$

where

$$N = N(s, t) = \int_{A(s)} \sigma^{11}(1 + \kappa z)\mathrm{d}A$$

$$Q = Q(s, t) = \int_{A(s)} \sigma^{12}\,\mathrm{d}A \tag{27}$$

$$M = M(s, t) = \int_{A(s)} \sigma^{11}(1 + \kappa z)z\,\mathrm{d}A$$

$$I_i(s) = \int_{A(s)} \rho z^i\mathrm{d}A \tag{28}$$

The quantities N, Q, M are called normal force, shearing-force and bending moment respectively (Fig. 2).

Integrating equation (25) by parts and referring to equation (20), the following equations of motion are obtained in terms of the foreces:

$$\begin{aligned} N' + \kappa Q + p_s &= I_0\ddot{u} + I_1\ddot{\Phi} \\ -\kappa N + Q' + p_N &= I_0\ddot{w} \\ M' - Q &= I_1\ddot{u} + I_2\ddot{\Phi} \end{aligned} \tag{29}$$

Boundary conditions

With given stresses $\overset{*}{\sigma}{}^{11}$ and $\overset{*}{\sigma}{}^{12}$ acting at an end of the beam, the resultant force per unit area is:

$$\mathbf{F} = \overset{*}{\sigma}{}^{11}\mathbf{e}_1 + \overset{*}{\sigma}{}^{12}\mathbf{e}_2 = \overset{*}{\sigma}{}^{11}(1 + \kappa z)\mathbf{T} + \overset{*}{\sigma}{}^{12}\mathbf{N} \tag{30}$$

Denoting by a subscript l all magnitudes to be evaluated at that end of the beam, the external virtual work of the boundary forces is:

$$EVW_l = \int_{A(l)} \mathbf{F}_l\delta\mathbf{y}_l\,\mathrm{d}A = \overset{*}{N}_l\delta u_l + \overset{*}{M}_l\delta\Phi_l + \overset{*}{Q}_l\delta w_l \tag{31}$$

where $\overset{*}{N}_l$, $\overset{*}{M}_l$, $\overset{*}{Q}_l$ are related to the given stresses $\overset{*}{\sigma}{}^{11}$, $\overset{*}{\sigma}{}^{12}$ through equations (27).

Substituting the boundary values obtained from equation (25), the following conditions (or their linear combinations) can be prescribed independently at the boundaries

$$
\begin{aligned}
u_l &= \overset{*}{u}_l \quad \text{or} \quad N_l = \overset{*}{N}_l \\
w_l &= \overset{*}{w}_l \quad \text{or} \quad Q_l = \overset{*}{Q}_l \\
\Phi_l &= \Phi_l^* \quad \text{or} \quad M_l = \overset{*}{M}_l
\end{aligned}
\tag{32}
$$

where $\overset{*}{u}_l$, $\overset{*}{w}_l$, Φ_l^* are prescribed displacements at the boundary.

Constitutive equations

Let the stress-strain relation be given by:

$$
\begin{aligned}
\sigma^{11} &= E(s,z)E_{11} \\
\sigma^{12} &= 2G(s,z)E_{12}
\end{aligned}
\tag{33}
$$

where E and G are the moduli of elasticity and shear respectively.

Substituting equations (33) in (19) and the result in (27), the following expressions are obtained for the internal forces in terms of the displacements:

$$
\begin{aligned}
N &= C_0(u' + \kappa w) + C_1(\Phi' + \kappa u' + \kappa^2 w) + C_2 \kappa \Phi' \\
Q &= D(\Phi + w' - \kappa u) \\
M &= C_1(u' + \kappa w) + C_2(\Phi' + \kappa u' + \kappa^2 w) + C_3 \kappa \Phi'
\end{aligned}
\tag{34}
$$

where

$$
\begin{aligned}
C_i &= C_i(s) = \int_{A(s)} E(s,z) \cdot (1 + \kappa z) z^i \mathrm{d}A \\
D &= D(s) = \int_{A(s)} G(s,z) \mathrm{d}A.
\end{aligned}
\tag{35}
$$

Note that equations (34) can be rewritten as:

$$
\begin{aligned}
N - \kappa M &= K_0(u' + \kappa w) + K_1 \Phi' \\
M &= K_1(u' + \kappa w) + K_2(\Phi' + \kappa u' + \kappa^2 w) \\
Q &= D(\Phi + w' - \kappa u)
\end{aligned}
\tag{36}
$$

where

$$
\begin{aligned}
K_0 &= C_0 - \kappa^2 C_2 \\
K_1 &= C_1 - \kappa^2 C_3 \\
K_2 &= C_2 + \kappa C_3.
\end{aligned}
\tag{37}
$$

Note also that the axis can be chosen so as to make either I_1 or K_1 vanish.

3. NUMERICAL ANALYSIS

Substituting equation (34) in (29), the following expressions are obtained for the equations of motion in terms of the displacements:

$$[C_0(u' + \kappa w) + C_1(\Phi' + \kappa u' + \kappa^2 w) + C_2 \kappa \Phi']' + \kappa D(\Phi + w' - \kappa u) + p_s = I_0 \ddot{u} + I_1 \ddot{\Phi} \tag{38}$$

$$-\kappa [C_0(u' + \kappa w) + C_1(\Phi' + \kappa u' + \kappa^2 w) + C_2 \kappa \Phi'] + [D(\Phi + w' - \kappa u)]' + p_N = I_0 \ddot{w} \tag{39}$$

$$[C_1(u' + \kappa w) + C_2(\Phi' + \kappa u' + \kappa^2 w) + C_3 \kappa \Phi']' - D(\Phi + w' - \kappa u) = I_1 \ddot{u} + I_2 \ddot{\Phi} \tag{40}$$

In the same way the boundary conditions (32) can be expressed in terms of the displacements as follows:

$$\begin{aligned} u_l &= \overset{*}{u}_l \quad \text{or} \quad [C_0(u' + \kappa w) + C_1(\Phi' + \kappa u' + \kappa^2 w) + C_2\kappa\Phi']_l = \overset{*}{N}_l \\ w_l &= \overset{*}{w}_l \quad \text{or} \quad [D(\Phi + w' - \kappa u)]_l = \overset{*}{Q}_l \\ \Phi_l &= \overset{*}{\Phi}_l \quad \text{or} \quad [C_1(u' + \kappa w) + C_2(\Phi' + \kappa u' + \kappa^2 w) + C_3\kappa\Phi']_l = \overset{*}{M}_l \end{aligned} \tag{41}$$

The set of second-order partial differential equations (38–40) with boundary conditions (41) lends itself to application of Houbolt's method [4], with the set of ordinary differential equations to be solved, for each time step treated, by the finite-differences method (see next section).

Houbolt's method

For the sake of completeness, and also with a view of formulating the initial conditions in the most general form, Houbolt's method [4] is recapitulated below.

The equations of motion (38–40) can be written in matrix form as:

$$[L]\{\bar{u}\} = [\bar{M}]\{\ddot{u}\} - \{\bar{p}\} \tag{42}$$

where

$[L]$ a 3×3 linear differential operator
$[\bar{M}]$ a 3×3 mass matrix
} (both time-independent)

$$\{\bar{u}\} = \begin{Bmatrix} u \\ w \\ \Phi \end{Bmatrix}$$

$$\{\bar{p}\} = \begin{Bmatrix} p_s \\ p_N \\ 0 \end{Bmatrix}.$$

Next, a net of points is defined along the time coordinate. For any given point i of the net, the second time-derivative is expressed as that of a polynomial of n-th degree passing through the values of $\{\bar{u}\}$ at the n + 1 points $i, i-1, \ldots, i-n$ of the net.

Equation (42) can then be replaced by the following approximate expression:

$$[L]\{\bar{u}\}_i = [\bar{M}] \cdot \left(\alpha\{\bar{u}\}_i + \sum_{k=1}^{n} \beta_k\{\bar{u}\}_{i-k}\right) - \{\bar{p}\}_i \tag{43}$$

where

α, β_k: coefficients depending on the degree of the polynomial and the spacing of the points.
$\{\bar{u}\}_i$: the value of $\{\bar{u}\}$ at time point i.
$\{\bar{p}\}_i$: the value of $\{\bar{p}\}$ at time point i.

Rewriting equation (43) as:

$$([L] - \alpha[\bar{M}]) \cdot \{\bar{u}\}_i = [\bar{M}] \sum_{k=1}^{n} \beta_k\{\bar{u}\}_{i-k} - \{\bar{p}\}_i \tag{44}$$

it becomes evident that if the solution is known for the n preceding points in time, the solution for time i is obtainable by solving the set of ordinary differential equations (44), in which the right and left-hand sides may be viewed, respectively, as modifications of the external loading and of the actual stiffness properties of the structure. The boundary conditions to be applied are the original ones for time i.

Houbolt's method may thus be described as an implicit procedure permitting solution of a dynamic phenomenon as a series of successive modified statical problems. The most common choice for the degree of the polynomial is $n = 3$. For this case, and for a uniform net (constant time interval Δt), it has been shown[5] that the algorithm is stable irrespective of the value of Δt. The choice of Δt may, therefore, be based on accuracy considerations only, an advantage over explicit methods where the magnitude of Δt is subject to stability criteria.

For $n = 3$ and a constant Δt the following values are obtained for α and β_k:

$$\begin{aligned} \alpha &= 2/\Delta t^2 \\ \beta_1 &= -5/\Delta t^2 \\ \beta_2 &= 4/\Delta t^2 \\ \beta_3 &= -1/\Delta t^2 \end{aligned} \tag{45}$$

It is readily seen that for the first $n-1$ steps of the procedure, not all data required for evaluation of the right-hand side of equation (44) are available.

This shortage is remedied by the initial conditions. Let $\{\bar{u}\}_0$ and $\{\dot{\bar{u}}\}_0$ represent the known initial displacements and velocities. Then, for $n = 3$ and for a constant Δt, a polynomial through points $t_0 + \Delta t$, t_0, $t_0 - \Delta t$ and $t_0 - 2\,\Delta t$ allows to obtain the following expressions for the initial velocities and accelerations respectively:

$$\{\dot{\bar{u}}\}_0 = \frac{1}{6\Delta t}[2\{\bar{u}\}_1 + 3\{\bar{u}\}_0 - 6\{\bar{u}\}_{-1} + \{\bar{u}\}_{-2}] \tag{46}$$

$$\{\ddot{\bar{u}}\}_0 = \frac{1}{\Delta t^2}[\{\bar{u}\}_1 - 2\{\bar{u}\}_0 + \{\bar{u}\}_{-1}] \tag{47}$$

where $\{\bar{u}\}_{-1}$ and $\{\bar{u}\}_{-2}$ are fictitious values at times $t_0 - \Delta t$ and $t_0 - 2\Delta t$, t_0 being the initial time.

The initial acceleration is linearly related to the initial displacements and loads through equation (42). Accordingly, equations (46, 47) yield $[\bar{M}]\{\bar{u}\}_{-1}$ and $[\bar{M}]\{\bar{u}\}_{-2}$ as linear combinations of $\{\bar{u}\}_0$, $\{\bar{u}\}_1$ and $\{\bar{p}\}_0$. Equation (44) can therefore be used for the first two steps of the procedure.

The final algorithm reads:

For $i = 1$ (time $t_0 + \Delta t$):

$$\left([L] - \frac{6}{\Delta t^2}[\bar{M}]\right)\cdot\{\bar{u}\}_1 = -\left(2[L] + \frac{6}{\Delta t^2}[\bar{M}]\right)\cdot\{\bar{u}\}_0 - \frac{6}{\Delta t}[\bar{M}]\{\dot{\bar{u}}\}_0 - 2\{\bar{p}\}_0 - \{\bar{p}\}_1. \tag{48}$$

For $i = 2$ (time $t_0 + 2\Delta t$):

$$\left([L] - \frac{2}{\Delta t^2}[\bar{M}]\right)\cdot\{\bar{u}\}_2 = -\frac{4}{\Delta t^2}[\bar{M}]\{\bar{u}\}_1 - \left([L] - \frac{2}{\Delta t^2}[\bar{M}]\right)\{\bar{u}\}_0 - \{\bar{p}\}_2 - \{\bar{p}\}_0. \tag{49}$$

For $i \geq 3$ (time $t_0 + i\Delta t$):

$$\left([L] - \frac{2}{\Delta t^2}[\bar{M}]\right)\{\bar{u}\}_i = \frac{1}{\Delta t^2}[\bar{M}]\cdot(-5\{\bar{u}\}_{i-1} + 4\{\bar{u}\}_{i-2} - \{\bar{u}\}_{i-3}) - \{\bar{p}\}_i. \tag{50}$$

Finite-difference scheme

Equations (38–40) possess the following feature, preserved also in the modified static equations of Houbolt's method: the first and the third equations do not contain the second s-derivative of w, while the second does not contain those of u and Φ. In these circumstances two distinct interlaced nets may conveniently be used-one for w and the other for u and Φ (Fig. 3), yielding a high degree of accuracy with relatively sparse nets[8].

For a constant increment Δs the following expressions for the numerical derivatives and unknowns are to be used in equations (38, 40):

$$\begin{aligned} &u''_j = (u_{j+1} - 2u_j + u_{j-1})/\Delta s^2; \quad u'_j = (u_{j+1} - u_{j-1})/2\Delta s; \quad u_j = u_j \\ &w'_j = (w_{j+1} - w_j)/\Delta s; \quad w_j = (w_{j+1} + w_j)/2 \\ &\Phi''_j = (\Phi_{j+1} - 2\Phi_j + \Phi_{j-1})/\Delta s^2; \quad \Phi'_j = (\Phi_{j+1} - \Phi_{j-1})/2\Delta s; \quad \Phi_j = \Phi_j \end{aligned} \tag{51}$$

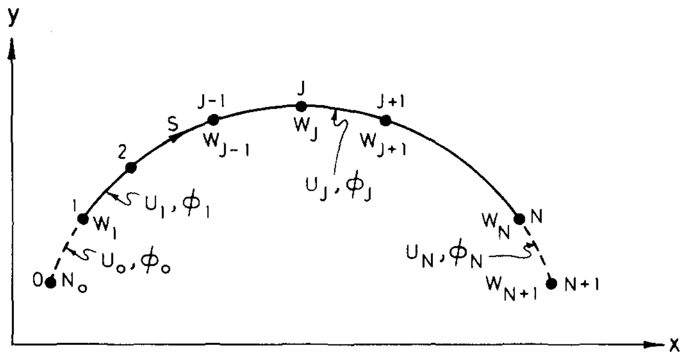

Fig. 3. Interlaced nets and corresponding unknowns.

and in Eq. (39):

$$
\begin{aligned}
&u'_j = (u_j - u_{j-1})/\Delta s; \quad u_j = (u_j + u_{j-1})/2 \\
&w''_j = (w_{j+1} - 2w_j - w_{j-1})/\Delta s^2; \quad w'_j = (w_{j+1} - w_{j-1})/2\Delta s; \quad w_j = w_j \\
&\Phi'_j = (\Phi_j - \Phi_{j-1})/\Delta s; \quad \Phi_j = (\Phi_j + \Phi_{j-1})/2
\end{aligned}
\tag{52}
$$

Further improvement in accuracy is obtainable by evaluating the derivative of *a* product directly instead of expanding it as a sum of two products[9]. For example, the derivative $(Dw')'$ in equation (39) is evaluated as:

$$
\begin{aligned}
(Dw')'_j &= \frac{1}{2\Delta s}[(Dw')_{j+1/2} - (Dw')_{j-1/2}] = \frac{1}{2\Delta s}\left\{D_{j+1/2}\frac{w_{j+1} - w_j}{\Delta s} - D_{j-1/2}\frac{w_j - w_{j-1}}{\Delta s}\right\} \\
&= \frac{1}{\Delta s^2}\{D_{j+1/2}w_{j+1} - (D_{j+1/2} + D_{j-1/2})w_g + D_{j-1/2}w_{j-1}\}
\end{aligned}
\tag{53}
$$

instead of:

$$
(Dw')'_j = D'_j w'_j + D_j w''_j = D'_j\frac{w_{j+1} - w_{j-1}}{2\Delta s} + D_j\frac{w_{j+1} - 2w_j + w_{j-1}}{\Delta s^2}
\tag{54}
$$

Solution of equations

With the unknowns and their s-derivatives formulated as per equations (51) and (52), the equations of motion and boundary conditions at time *i* constitute a set of linear algebraic equations.

Because of the high concentration of non-vanishing terms near the main diagonal of the coefficient matrix the set is conveniently solved by partitioning the coefficient matrix into a tridiagonal submatrix arrangement and applying the generalization of Potter's method[10] described in[11].

It should be noted that while the right-hand side of the set varies with time, the coefficient matrix remains the same after the second time step (see Eqs. (49) and (50)).

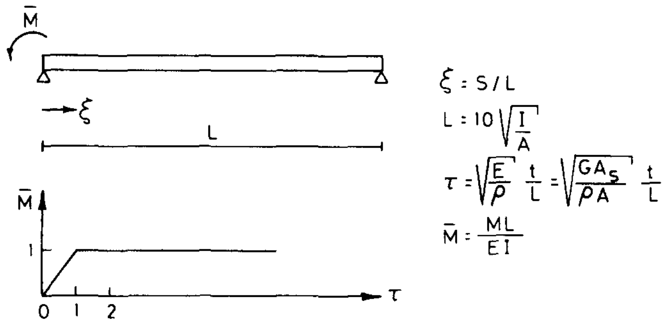

Fig. 4. Simply supported beam subjected to a ramp-platform moment at $\xi = 0$.

4. NUMERICAL RESULTS

A computer program was worked out according to the procedure outlined in the preceding section, and several examples were run on an IBM 370–165. Some of the results were compared with available data by other methods.

The first example—a beam (Fig. 4)—was worked out for comparison with the solution in [2],

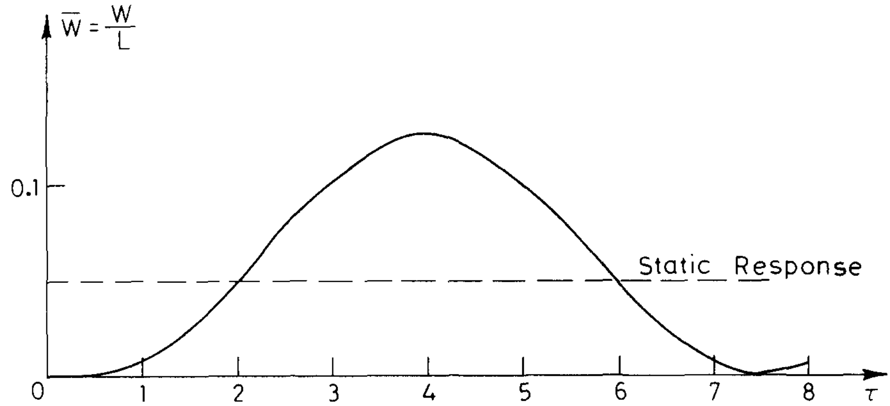

Fig. 5. Nondimensional deflection at the center ($\xi = 0{\cdot}5$).

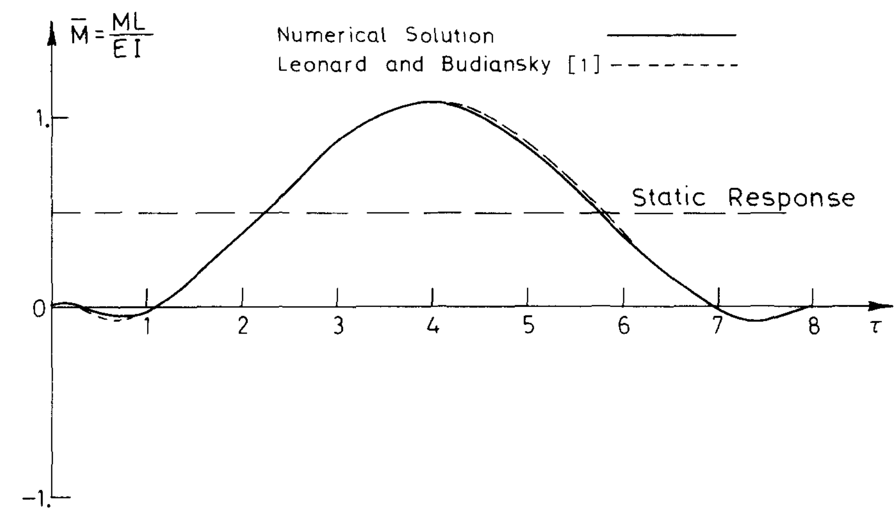

Fig. 6. Nondimensional moment at the center ($\xi = 0{\cdot}5$).

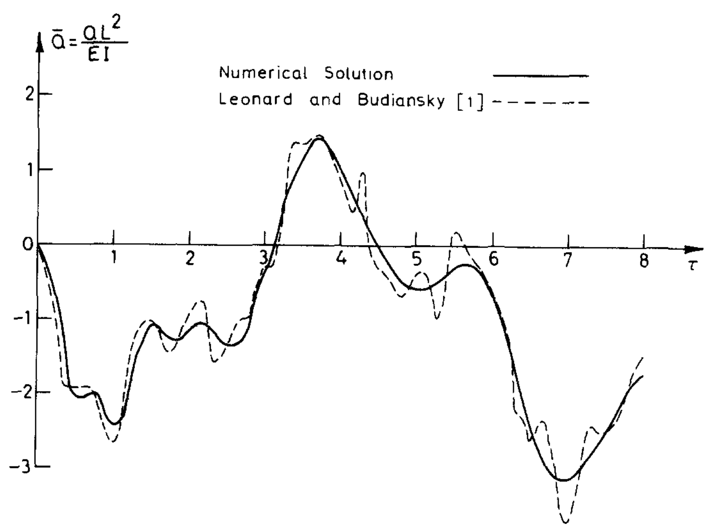

Fig. 7. Nondimensional shear force at the end $\xi = 0$.

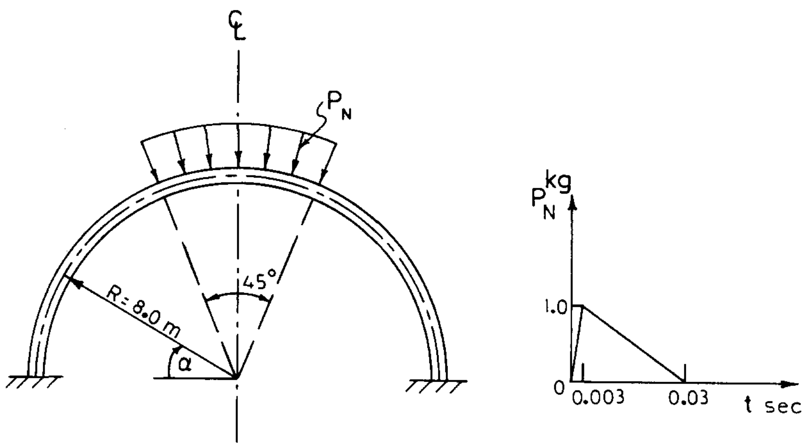

Fig. 8. Circular arch under triangular normal load.

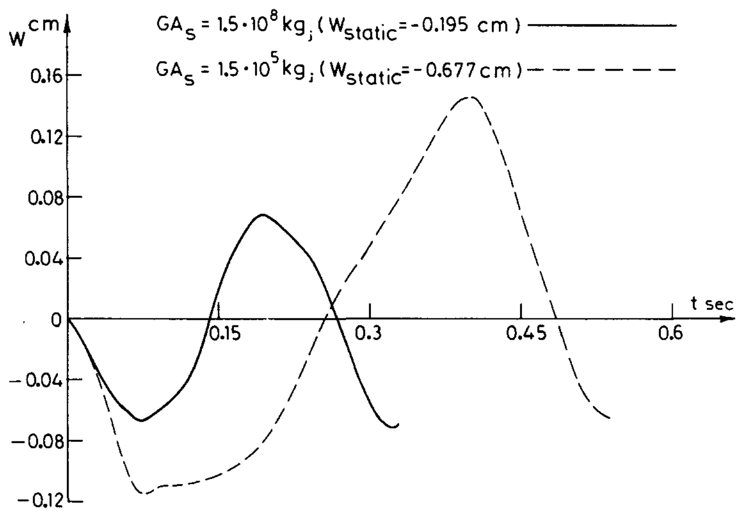

Fig. 9. Normal displacement at the center ($\alpha = 90°$).

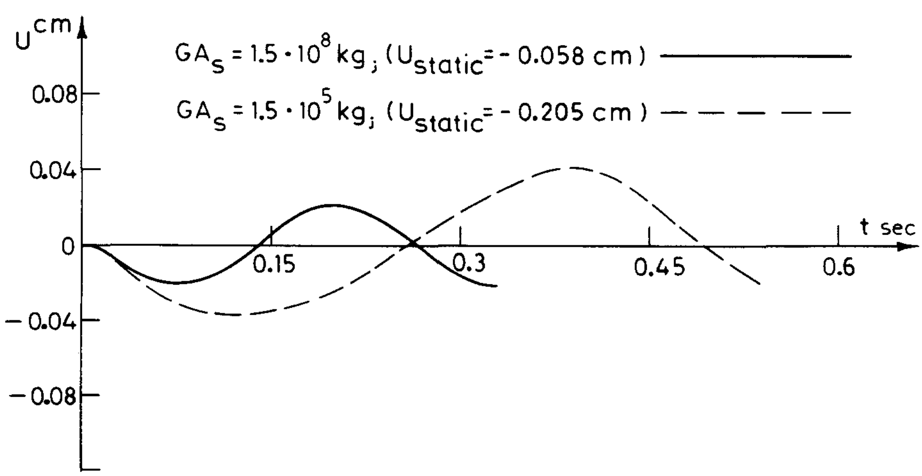

Fig. 10. Tangential displacement at $\alpha = 67{\cdot}5°$.

obtained by the characteristics method. All data and results are dimensionless. The number of location- and time differences was chosen as 21 and 100 respectively, with the time interval taken as 1/100 of the period of first natural mode of the beam. The midspan deflection and moment and the left end shearing force are plotted against time in Figs. (5, 6, 7) together with their counterparts in[2]. The graphs show good agreement-except for the shear diagram, where the obtained solution apparently averages the fluctuations in[2].

The second example is a circular arch under a dynamic load (Fig. 8) with the following parameters: in-plane rigidity $EA = 4 \times 10^8$ kg, bending rigidity $EI = 133 \times 10^8$ kg cm^2, mass density $\rho = 0{\cdot}24 \times 10^{-5}$ kg sec^2/cm^4. In order to bring out the contribution of the shear deformation, the example was worked out for two levels: $GA_s = 1{\cdot}5 \times 10^8$ kg and $1{\cdot}5 \times 10^5$ kg. The number of location differences for half the arch ($0 \leq \alpha \leq 90°$) was 41, and the time interval $-1/100$ of the period of first natural mode for the higher GA_s level and 1/200 for the lower one.

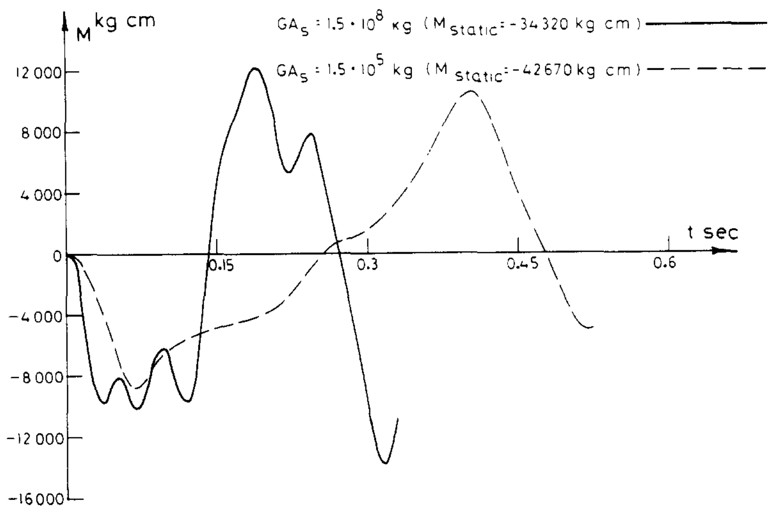

Fig. 11. Bending moment at the center ($\alpha = 90°$).

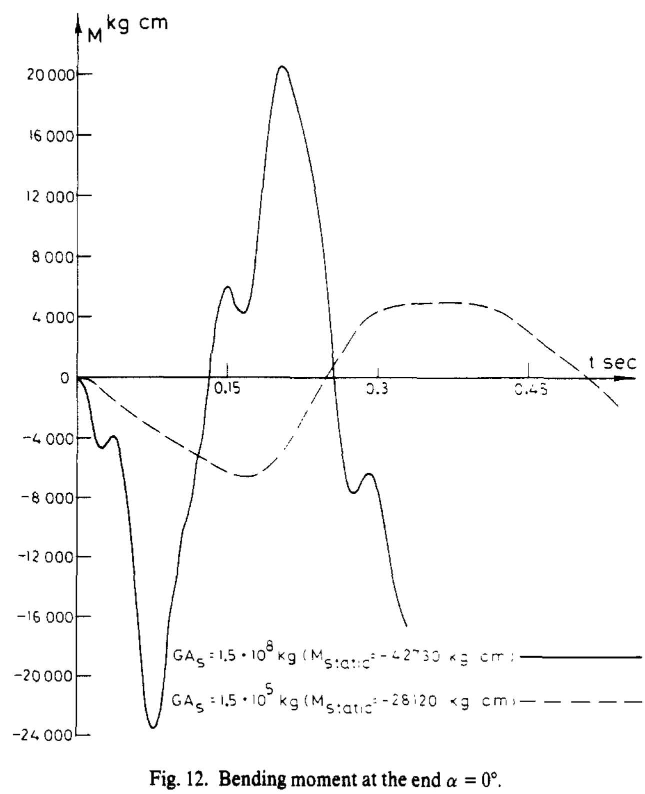

Fig. 12. Bending moment at the end $\alpha = 0°$.

Deflections, moments, axial forces and shearing forces for the two GAs levels are plotted against time in Figs. 9 trough 14, which also include the statical results for comparison. The contribution of the shear deformation is seen to be substantial.

5. SUMMARY AND CONCLUSIONS

A linear theory, admitting shear deformations and rotary inertia, and a solution procedure are presented for an arbitrary plane curved beam subjected to arbitrary static and dynamic loads. The equations of motion with the displacements and total rotation as unknowns are converted to finite difference equations and solved by Houbolt's method. The proposed method may be extended, with the aid of suitable continuity equations, to systems consisting of several curved beams of different shapes.

The second numerical example shows that the contribution of the shear deformation is substantial, and in dynamical problems actually results in a basically different solution.

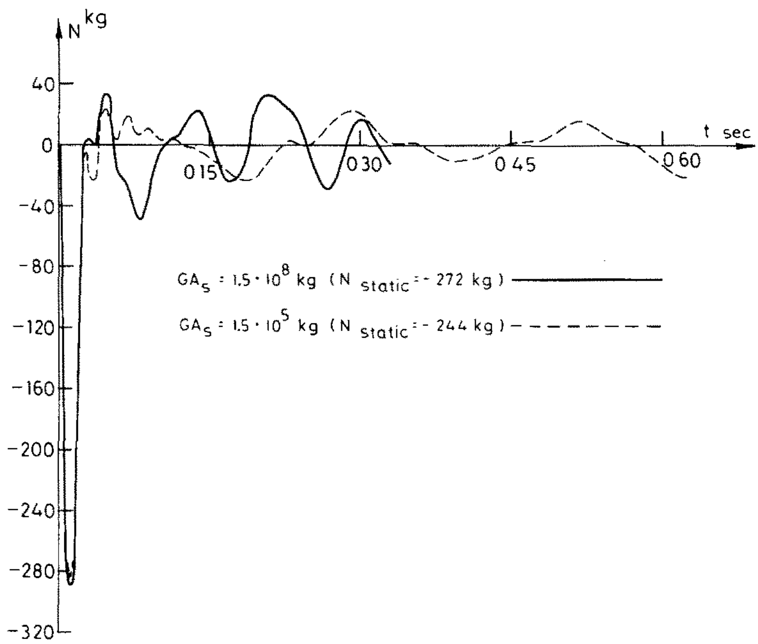

Fig. 13. Axial force at the center ($\alpha = 90°$).

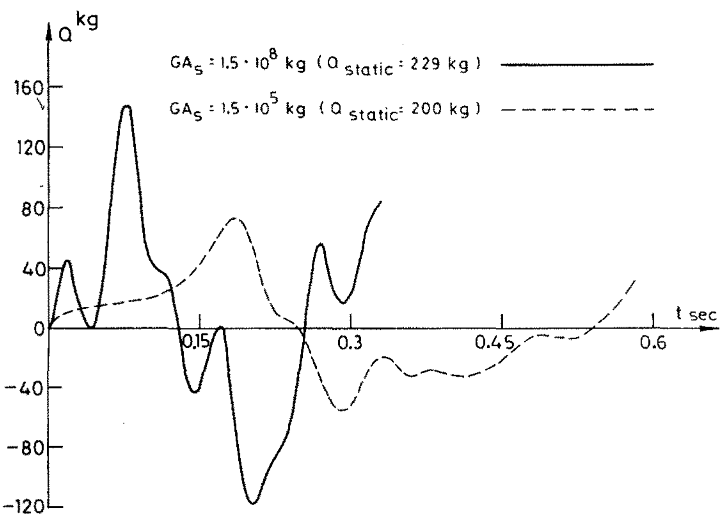

Fig. 14. Shear force at the end $\alpha = 0°$.

REFERENCES

1. S. Timoshenko, *Vibration Problems in Engineering*. 2nd Edn., pp. 337–338. Van Nostrand, Amsterdam (1937).
2. R. W. Leonard and B. Budiansky, *On travelling waves in beams*. NACA Langley Aeronautical Laboratory, Report 1173 (1955).
3. R. W. Leonard, *On solutions for the transient response of beams*. NASA Technical Report R-21 (1959).
4. J. C. Houbolt, A recurrence matrix solution for the dynamic response of elastic aircraft. *J. Aeronaut. Sci.* **17**, 540 (1950).
5. D. E. Johnson, A proof of the stability of the Houbolt method. *AIAA Journal* 1450 (August 1966).
6. Y. Tene, *A complete first approximation linear shell theory admitting shear deformation*. Technion, Faculty of Civil Eng., Publ. no. 116, Haifa, (June 1968); also *TSGB Matrix Tensor Quart.* **21**, (1970).
7. Y. Tene and I. Sheinman, Analysis of skew plates with shear deformation using natural coordinates. *ASCE, J. Mech. Div.* to be published.
8. A. K. Noor and V. K. Khassdelwal, *Improved finite-difference variant for the bending analysis of arbitrary cylindrical shells*. Unicif Report No. R-58, University of New South Wales, Kensington, Australia (1969).
9. N. J. Cyrus and R. E. Fulton, Finite-difference accuracy in structural analysis. *Proc. ASCE, J. Str. Div.* **92**, No. ST6 (Dec. 1966).
10. M. L. Potters, *A matrix method for solution of a linear second order difference equation in two variables*. Report NR-19, Mathematisch Centrum, Amsterdam (1955).
11. Y. Tene, M. Epstein and I. Sheinman, A generalization of Potter's method. *Computers and Structures* to be published.